ARL-TN-1199 ● APR 2024

Solvent-Free Mechanochemical Synthesis of Lead-Free Piezoelectric Perovskite Potassium Sodium Niobate Incorporated with Tungsten

by Latha Nataraj, Anthony Roberts, Scott Walck, Tucker Moore, and Kristopher Darling

NOTICES

Disclaimers

The findings in this report are not to be construed as an official Department of the Army position unless so designated by other authorized documents.

Citation of manufacturer's or trade names does not constitute an official endorsement or approval of the use thereof.

Destroy this report when it is no longer needed. Do not return it to the originator.

ARL-TN-1199 ● APR 2024

Solvent-Free Mechanochemical Synthesis of Lead-Free Piezoelectric Perovskite Potassium Sodium Niobate Incorporated with Tungsten

Latha Nataraj, Anthony Roberts, Tucker Moore, and Kristopher Darling
DEVCOM Army Research Laboratory

Scott Walck
SURVICE Engineering

REPORT DOCUMENTATION PAGE

1. REPORT DATE	2. REPORT TYPE	3. DATES COVERED	
		START DATE	END DATE
April 2024	Technical Report	1 October 2022	30 September 2023

4. TITLE AND SUBTITLE
Solvent-Free Mechanochemical Synthesis of Lead-Free Piezoelectric Perovskite Potassium Sodium Niobate Incorporated with Tungsten

5a. CONTRACT NUMBER	5b. GRANT NUMBER	5c. PROGRAM ELEMENT NUMBER
5d. PROJECT NUMBER	**5e. TASK NUMBER**	**5f. WORK UNIT NUMBER**

6. AUTHOR(S)
Latha Nataraj, Anthony Roberts, Scott Walck, Tucker Moore, and Kristopher Darling

7. PERFORMING ORGANIZATION NAME(S) AND ADDRESS(ES)
DEVCOM Army Research Laboratory
ATTN: FCDD-RLA-VB
Aberdeen Proving Ground, MD 21005

8. PERFORMING ORGANIZATION REPORT NUMBER
ARL-TN-1199

9. SPONSORING/MONITORING AGENCY NAME(S) AND ADDRESS(ES)	10. SPONSOR/MONITOR'S ACRONYM(S)	11. SPONSOR/MONITOR'S REPORT NUMBER(S)

12. DISTRIBUTION/AVAILABILITY STATEMENT
DISTRIBUTION STATEMENT A. Approved for public release: distribution unlimited.

13. SUPPLEMENTARY NOTES
ORCID IDs: Tucker Moore, 0009-0000-9646-8465; Latha Nataraj, 0000-0001-5041-8809

14. ABSTRACT
A quest for nontoxic alternatives to conventional lead-based ferroelectric and piezoelectric materials led to avid research in complex perovskite oxides and systems characterized by morphotropic phase boundary due to the abrupt increase in the dielectric and piezoelectric constants occurring in this region. Niobate perovskites like the (K, Na) NbO_3 (KNN) family have emerged as some of the most important lead-free ferroelectric and piezoelectric materials. Engineering of facile, economical, and environmentally safe synthesis methods for such materials poses challenges to ensuring chemical homogeneity and achieving desired structures. Here, we report solvent-free mechanochemical synthesis of single-phase lead-free piezoelectric perovskite oxide (W-KNN) of KNN incorporated with tungsten, using a simple high-energy ball-milling process with shorter processing times and lower calcination temperatures than those reported in literature. The characterization of the derived powder confirms the structure, morphology, crystallinity, and chemical composition of the synthesized material. The presented method could also pave the way for a rapid, facile, and faster synthesis mechanism at lower processing temperatures for other promising functional oxides.

15. SUBJECT TERMS
Mechanical Sciences, Sciences of Extreme Materials, stimuli-responsive, multifunctional, environmentally friendly, nontoxic, bio-compatible piezoelectric material

16. SECURITY CLASSIFICATION OF:			17. LIMITATION OF ABSTRACT	18. NUMBER OF PAGES
a. REPORT	b. ABSTRACT	C. THIS PAGE		
UNCLASSIFIED	UNCLASSIFIED	UNCLASSIFIED	UU	26

19a. NAME OF RESPONSIBLE PERSON	19b. PHONE NUMBER *(Include area code)*
Latha Nataraj	(410) 278-3814

STANDARD FORM 298 (REV. 5/2020)
Prescribed by ANSI Std. Z39.18

Contents

List of Figures

List of Tables

1. Introduction

High-performance piezoelectric materials are widely used in electronics such as sensors, actuators, transducers, transformers, to name a few. Therefore, the research in this class of materials has been at the forefront of technology for decades. Since the 1950s, $PbZr_{(1-x)}Ti_xO_3$ (PZT)-based materials have received great interest due to their excellent piezoelectric properties resulting in their extensive use in various piezoelectric devices. However, with PZT containing greater than 60% toxic lead, it is highly detrimental to human health and environment from preparation and processing to end-of-life disposal. Therefore, there has been increasing interest in lead-free piezoceramics. Among the lead-free piezoelectric compositions, potassium sodium niobate (K, Na) NbO_3, also known as KNN, is considered promising[1] to replace PZT, as it has a high curie temperature and relatively strong piezoelectricity due to the abrupt increase in the dielectric and piezoelectric constants at the morphotropic phase boundary. Typically, such materials have been synthesized using slow, cumbersome sol-gel methods or elaborate solid-state reaction processes with several intricate processing steps, long mixing and grinding times of the reactant powders, multiple and prolonged calcination steps at high temperatures, and intermediate wet milling processes.[2–5] Also, the volatility of Na and K at elevated temperature and the sensitivity of the compound to moisture make it difficult to obtain dense and well-sintered KNN ceramic by conventional sintering.[6–9] Developing facile, economical, and environmentally safe routes for the synthesis of single-phase perovskite oxides pose challenges to ensuring chemical homogeneity and desired structures.[10,11]

Mechanochemistry seems to be gaining great interest due to its potential for solvent-free, direct-reaction, and low-temperature processing mechanisms for functional oxides,[12] providing a simple, sustainable, and highly energy-efficient synthesis route, typically using a milling technique. The possibility of promoting solid-state chemical reactions at room temperature triggered by mechanical stress, instead of heat, to overcome all thermodynamic reaction barriers offers great potential.[13–15] Over the past two decades, various functional oxides, including $BiFeO_3$,[16] (K, Na)NbO_3,[17,18] $KNbO_3$,[19] $NaNbO_3$,[18,20] $BaTiO_3$,[21,22] Pb(Mg, Nb)O_3-$PbTiO_3$,[23,24] Pb(Mg, Nb)O_3,[25–28] (Pb, La)(Zr, Ti)O_3,[29,30] Pb(Zr, Ti)O_3,[31–33] $PbZrO_3$,[34] and $PbTiO_3$,[35] have been synthesized using milling techniques. Achieving the stabilization of a single-phase perovskite using cost-effective micron-scale reactant powders through rapid solid-state synthesis methods presents a significant challenge. Conventional approaches involving extended milling times spanning tens to hundreds of hours, have proven ineffective in inducing fundamental chemical transformations. Instead, these extended milling periods

often result in the formation of nanocrystalline or amorphous reactant powders contaminated with materials from the milling media. Research has shown that the mechanical stresses exerted by the milling media can alter the properties of the reactant powders, reducing both the required calcination temperature and processing time.[17,36,37] The milling time for nanocrystallization is greatly influenced by the particle size of the reactant materials,[38] which could be much lower with nanoscale reactant powders.[21] Also, the impacting energy and frequency of the milling process determine the cumulative kinetic energy transferred to the reactant powder mixture to facilitate the mechanochemical reaction.

Lee et al.[39] established that the total energy transferred to the powder afforded by planetary mills was typically less than approximately 35 kJ/g for 1 h of milling, depending on design of the mill, the milling medium, the milling speed, and other related factors. Through a correlation of the inherent activation energy barrier in the reaction system with the energy transferred to the reactant powder per impact and the frequency of impacts, a perspective emerges: a mechanochemical reaction with a higher activation energy necessitates a more energetic milling condition for success. In response to this insight, the researchers adapted a planetary ball mill to impart increased energy, thereby expediting the process when employing micron-scale reactant powders. This modification enabled the swift synthesis of a single-phase KNN through a high-rate mechanochemical reaction, with remarkably short milling times, as brief as 20 min. This rapid process indicated the formation of the perovskite structure.[39] Chemical modifications of KNN and other lead-free piezoelectric materials pose major challenges.[40]

In this study, we present an uncomplicated and speedy method for synthesizing a perovskite oxide, specifically lead-free piezoelectric perovskite oxides known as W-KNN. This method employs a high-rate mechanochemical reaction conducted through a straightforward, solvent-free, high-energy ball-milling process. What sets this process apart is its ability to achieve the desired results with significantly reduced processing times and lower calcination temperatures when compared to previously documented procedures in the literature. The synthesized W-KNN was characterized using differential scanning calorimetry (DSC), X-ray diffraction (XRD), scanning electron microscopy (SEM), transmission electron microscopy (TEM), and energy-dispersive X-ray spectroscopy (XEDS). Further, the powder was pressed into compacts of 6 mm diameter and thickness of approximately 1.4 mm for characterization of electrical and piezoelectric properties.

2. Methods

2.1 Materials

The reactants used in this study were K_2CO_3 (≥99.0%, ~150 μm, Sigma-Aldrich), Na_2CO_3 (≥99.5%, ~10 μm, Sigma-Aldrich), Nb_2O_5 (99.9%, ~2 μm, Sigma-Aldrich), as typically used in a conventional synthesis of KNN. Owing to their hygroscopic characteristics, handling these powders, including the act of weighing and loading the milling vial, were carefully performed within a glove box in an Argon (Ar) atmosphere. A tungsten carbide (WC) vial with WC milling media were used for milling and a stoichiometric K_2CO_3-Na_2CO_3-Nb_2O_5 powder mixture was used for the syntheses of W-KNN. The general chemical reaction of the KNN is as follows:

$$0.25\ K_2CO_3 + 0.25\ Na_2CO_3 + 0.5\ Nb_2O_5 \rightarrow (K_{0.5}Na_{0.5})\ NbO_3 + 0.5\ CO_2 \qquad (1)$$

2.2 Material Synthesis

Mechanochemical reactions were conducted following the process by Lee et al.[39] using a Spex 8000M high-energy mixer/mill, instead of the modified planetary mill used in their process. The high-energy mill shown in Fig. 1a grinds the material with combined back-and-forth swings with short lateral movements, with the ends of the vial forming a figure eight. A WC vial and milling media 3/8 inch in diameter, shown in Fig. 1b, were used for the milling process. The vial was 4.2 cm in diameter D_v and 81.74 cm^3 in volume. The stoichiometric ratio of the reactants as calculated amounted to 0.8907 g of K_2CO_3, 0.6831 g of Na_2CO_3, and 3.4029 g of Nb_2O_5 to yield approximately 4.97 g of powder mixture, which was placed in the WC vial with the WC milling media (density = 15.1 g/cm^3). Close to the work by Lee et al.[39] that uses the dry milling technique to synthesize KNN, the ball-to-powder weight ratio was kept at 36:1, amounting to 23 balls. All powders were stored, weighed, and loaded into the vial inside the glovebox, in an Ar atmosphere. Five different milling times were explored: 5 min, 10 min, 20 min, 30 min, and 1 h, and the milled powders, as shown in Fig. 1c were analyzed for further processing.

(a) (b) (c)

Fig. 1 (a) High-energy ball mill, (b) WC vial and media, and (c) synthesized KNN powder

As demonstrated by established processes, the resulting powder mixtures need to be calcined to complete the mechanochemical reaction to achieve KNN. Calcination performed at a temperature of 850 °C for 6 h, which has worked in other processes such as Lee et al.,[39] did not render success in our process. Hence, we used thermogravimetric (TG) analysis and DSC to determine the right calcination temperature and duration to form KNN.

Each of the resultant milled powders studied for mass changes and thermal effects using TG analysis and DSC (with the NETZSCH STA 449 F3 Jupiter, shown in Fig. 2a) to determine the temperature of the onset of the mechanochemical reaction in the milled powders. Approximately 25 mg of the 60-min milled powder was placed in an alumina (Al_2O_3) crucible and heated to 850 °C at a rate of 10 °C/min in Ar atmosphere. Figure 2b shows the TG/DSC of the milled powder after heat treatment of the milled powder at 650 °C based on the determined calcination temperature from the DSC data. As all the reactant powders as well as the milled powders were handled and stored inside a glove box, we do not see the weight loss that can be attributed to water evaporation as seen in many TG plots. (However, we did notice it when we performed the same test on a sample left outside for a few days.) As seen from the DSC (blue) curve, the exothermic peak of the reaction forming the KNN begins at around 475 °C and ends around 650 °C. The drop in mass as indicated by the TG curve in this region is most likely caused by the loss of carbon dioxide as seen in Eq. 1, which stabilizes at approximately 650 °C indicating that the reaction is complete. So, the calcination temperature for the milled powder in this work was established to be around 650 °C, lower than the numbers of about 850 °C found in other processes.[39,41]

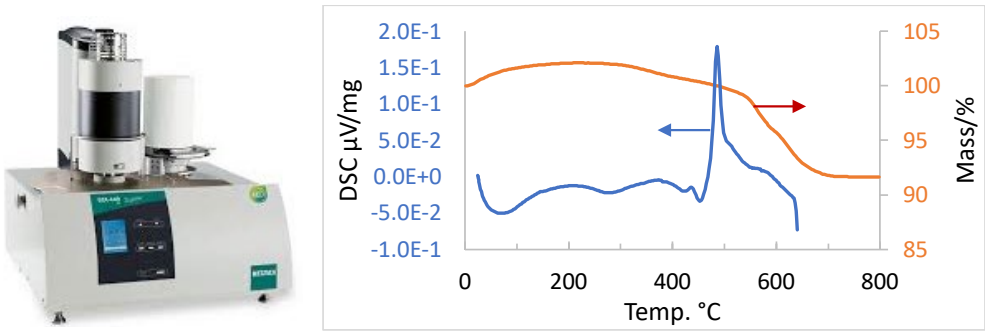

(a) (b)

Fig. 2 (a) NETZSCH STA 449 F3 Jupiter and (b) TG/DSC data for the 60-min milled powder

Therefore, the milled powder was calcined at 650 °C for 1 hh-, as a trial, in an Ar atmosphere in a Thermocraft tube furnace with an Al_2O_3 tube with the powder placed in an Al_2O_3 boat (Fig. 3). The structural characteristics of the calcined powders were then studied using XRD, SEM, TEM, and XEDS.

Fig. 3 Thermocraft tube furnace: the milled powder was calcined at 650 °C for 1 h with an Al_2O_3 tube with the powder placed in an Al_2O_3 boat

A small amount of the calcined powder was placed, as synthesized, on the sample holder of the XRD system to obtain the diffraction peaks. To avoid sample charging during SEM imaging, the samples are prepped by sprinkling the powder samples onto one side of small strips of double-sided sticky carbon tape. The other sticky side of the carbon tape is fixed onto the stub sample holder. Any sample particles not firmly affixed to the carbon tape was removed by blowing them away using pressurized nitrogen. For TEM, the sample was pressed by ultra-sonicating the calcined powder in acetone to overcome agglomeration and a drop of the sonicated suspension was dropped onto a copper grid, which was loaded into the TEM system once the acetone evaporated.

Next, to test the piezoelectric performance of the synthesized W-KNN, the powder was compressed into well sintered compacts with good density for good piezoelectric and ferroelectric properties. Following multiple experimental trials involving pressing and sintering at varying temperatures, we successfully applied established hot-pressing methods available in the US Army Combat Capabilities

Development Command Army Research Laboratory's (ARL's) Ceramic and Transparent Materials Branch. These methods were further enhanced through the process outlined by Rutkowski et al.[42]

First, 2.0123 g of the synthesized W-KNN powder with 60-min milling time was weighed out. A 1-inch-diameter cylindrical graphite die was coated uniformly with a slurry of hexagonal boron nitride (h-BN) and ethyl alcohol to act as a diffusion barrier for carbon between the graphite die and the part during hot pressing. Bharathi and Varma[43] demonstrated that h-BN helps with the stimulation of KNN densification process. After placing the coated die in an oven at 70 °C for 1 h to evaporate any traces of the ethyl alcohol from the coating, the W-KNN powder was placed between BN spacers, pressed with 8000 lbf three times, and held for 10 s each time to obtain a robust green compact. This was then transferred to an Oxygon benchtop refractory-metal hot press, which was evacuated to 10^{-5} torr, then backfilled with gettered ultrahigh purity Ar (<1 ppb O_2). The die was heated at 50 °C/min to 800 °C, held at 800 °C for 1 h, and then cooled at 50 °C/min to room temperature. A uniaxial load of 8000 lbf (70.3 MPa) was applied at the beginning of the 800°C hold and released at the end of the hold.

3. Results and Discussion

The structural phases of the calcined powder were characterized by an X-ray diffractometer (Malvern Panalytical's X'Pert Pro, UK) using Co Kα radiation at a power of 40 kV and 45 mA and at a scan speed of 1°/min. The calcined powder was also sent for chemical analysis using direct current (DC) plasma emission spectroscopy as per ASTM E 1097-12[44] at Luvac laboratories. The morphology of the sintered samples was studied using a Hitachi S-4700 cold field-emission scanning electron microscope with an operating voltage of 5 kV equipped with an Octane Elite Super X-ray energy-dispersive spectrometer (EDAX, Inc.). A transmission electron microscope (JEM-2100F; JEOL, Tokyo, Japan) with scanning transmission electron microscopy (STEM) capability and equipped with a windowless Octane T Optima XEDS detector (EDAX, Inc.) was also used for further study of the synthesized powder.

3.1 DC Plasma Emission Spectroscopy

The chemical analysis (DC plasma emission spectroscopy, Luvac), as per ASTM E 1097-12, on the calcined powder revealed traces of W in the sample.

Table 1 summarizes the results obtained. The powders obtained by 10-min (#9 KNN) and 60-min (#8 KNN) milling times showed 0.033 wt% (0.0051 at%) and 0.053 wt% (0.010021 at%) of W, respectively. This is expected since more W is introduced from the WC vial and milling media with longer milling times. The powder contained K, Na, and Nb from the stoichiometric reactants, and the oxygen concentration was determined by balance. Further studies are underway to determine W distribution in the sample.

Table 1 Results from the DC plasma emission spectroscopy of the mechanochemically synthesized calcined powder with milling times of 10 and 60 min

Element	At% 10 min	At% 60 min
Potassium	8.69	14.85
Sodium	9.16	15.72
Niobium	12.51	18.48
Tungsten	0.0051	0.0100
Oxygen balance	69.65	50.94

As shown in Table 2, the 10- and 60-min results show that the K/Na ratios are close to 1; however, the K and Na ratios to Nb indicate that there is a deficiency in Nb when compared to the formula, $(K_{0.5}Na_{0.5})\ NbO_3$. Ongoing efforts are underway to obtaining a more comprehensive chemical analysis of all the synthesized powders for the various milling times and understand the effects of the Nb deficiency.

Table 2 Ratios of the different elements calculated from the atomic percents of the results from the DC plasma emission spectroscopy of the synthesized KNN

Milling time	K/Na	k/Nb	Na/Nb
60 min	0.944	0.803	0.851
10 min	0.947	0.694	0.733

3.2 X-ray Diffraction (XRD)

Figure 4 shows the X-ray diffraction patterns of the mechanochemically synthesized stoichiometric K_2CO_3-Na_2CO_3-Nb_2O_5 powder as a function of the milling time, after a heat treatment 650 °C for 1 h. As the milling time increases from 5 to 10 min, the intensity of the Nb_2O_5 peaks rapidly decrease due to the reduced crystallite size of the pentoxide. Also, the intensity of the peaks from alkali metal carbonates, K_2CO_3 and Na_2CO_3, disappear over the same milling time interval. In addition, a slight increase of the background near the reflections likely due to disordering of the crystal structure.

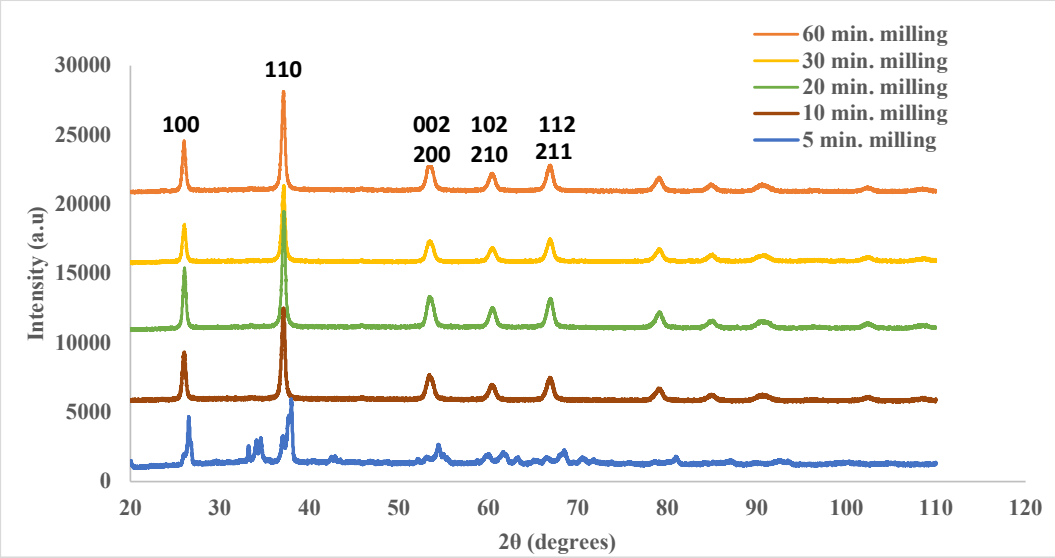

Fig. 4 X-ray diffraction patterns of the mechanochemically synthesized heat-treated stoichiometric milled powder with varying milling times

The oxide-assisted disordering/amorphization of carbonates during milling has been previously observed in X_2CO_3-Nb_2O_5 (X = K or/and Na) systems and has been understood to be due to the reconstruction of -CO_3^{2-} ions into a carbonate complex that results in a loss of long-range periodicity of the carbonates.[45] As depicted in Fig. 4, when the milling duration extends to 10 min and beyond, the characteristic peaks of Nb_2O_5 vanish. In their place, diffraction peaks arise, corresponding to a well-crystallized and single-phase material, identical to those in the work by Lee et al.[39] where it was indexed using Joint Committee on Powder Diffraction Standards (JCPDS) card no. 01-071-0946. However, we found that the composition of 01-071-0946 did not consist of K, so we looked in the JCPDS database for the correct match(es) for KNN and found those to be 04-025-7609 (Primary) with cross-references to 01-084-6855 (Alternate), 01-085-7128 (Alternate), 04-017-0216 (Alternate), and 04-025-8304 (Alternate). These peaks can be ascribed to the orthorhombic structure of the synthesized KNN powder. This observation also confirms that the 1-h heat treatment was adequate for the calcination step, which stands in stark contrast to the lengthier processes reported in other studies.[39,41]

3.3 Scanning Electron Microscopy (SEM)

The SEM micrographs of the KNN prepared by mechanochemical synthesis are as seen in Fig. 5 at lower and higher magnification. Images indicate well-developed grains with particle sizes in the range of tens to hundreds of nanometers.

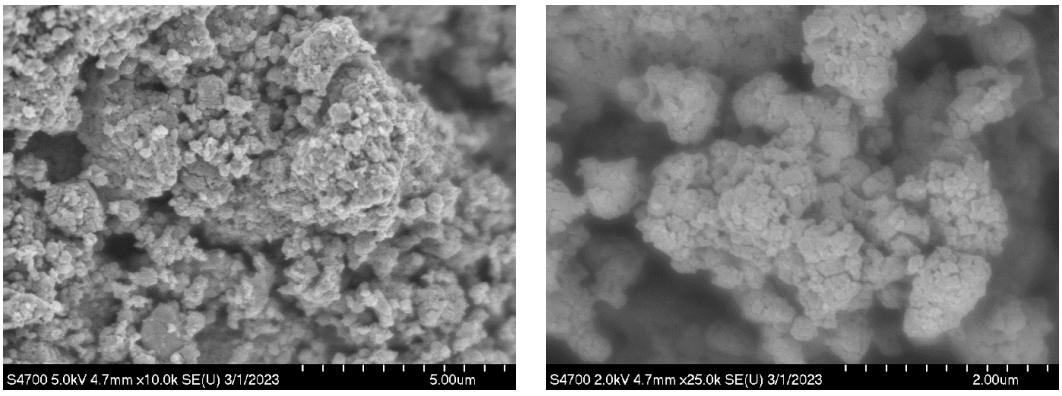

(a) (b)

Fig. 5 SEM micrographs of the sample with 60-min milling time at (a) lower and (b) higher magnification

3.4 Transmission Electron Microscopy (TEM)

Figure 6a shows a TEM bright-field micrograph of a group of the synthesized KNN particles. The examination of the particle under the TEM, as marked, confirms the size as tens to hundreds of nanometers as established by the SEM measurements. The selected area electron diffraction (SAED) pattern in Fig. 6b confirms the crystalline structure of the particles and was analyzed using CSpot software V2.2.0 and the Crystallography Open Database (COD),[46] CIF #2300499. There are 91 phases from the COD that match the diffraction pattern when the elements K, Na, O, and Nb are used in the search. Comparing just the first two JCPDS cards from the list in Section 3.2, the 01-084-6855 card is similar to 15 phases found in the COD, while the 01-085-7128 card is similar to 13. For all the JCPDS cards listed, the empirical formulae given were all $K_{0.5}Na_{0.5}NbO_3$. The elemental ratios of the cations from the formula are shown in Table 3. The list of COD phases had more variation in the chemistry. Of the 91 phases found in the COD, there were 61 phases having that or very nearly that of $K_{0.5}Na_{0.5}NbO_3$, while the rest had either ratios of lower K and higher Na to Nb or higher K and lower Na to Nb compared to the 0.5/0.5 ratio for K and Na in the $K_{0.5}Na_{0.5}NbO_3$ formula. Most of these were found in the ratio of either approximately 0.3/0.7 or 0.7/0.3 for K/Na, while a few phases had either very low K or very low Na.

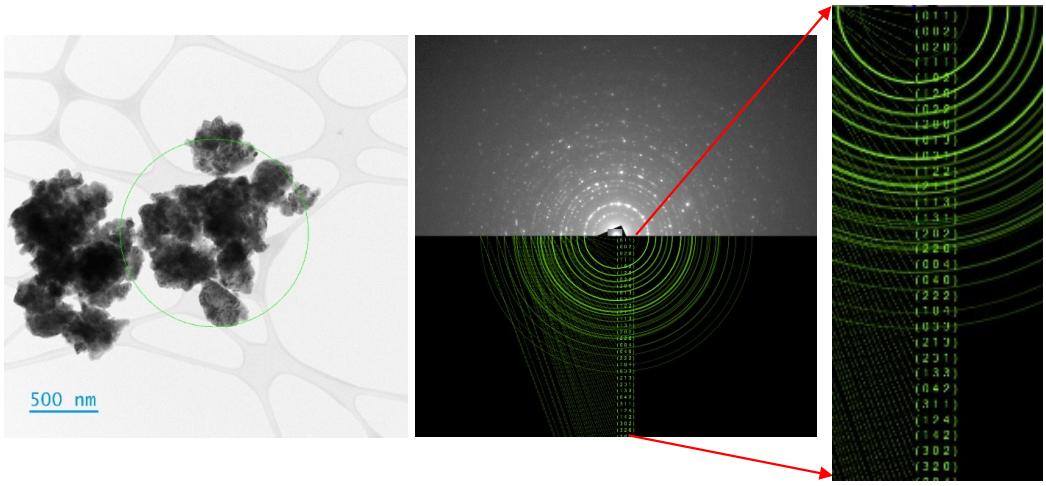

(a) (b)

Fig. 6 (a) TEM bright-field image of KNN particle and (b) SAED pattern of the synthesized powder with 60-min milling time

Table 3 Elemental ratio values for the formula, $K_{0.5}Na_{0.5}NbO_3$

Formula: $K_{0.5}Na_{0.5}NbO_3$		
K/Na	**K/Nb**	**Na/Nb**
1	0.5	0.5

3.5 Energy-Dispersive X-ray Spectroscopy (XEDS)

Figure 7 shows the spectrum from XEDS using the STEM, with well-defined peaks for Na, K, Nb, and O, as expected. Tungsten was not detected in the XEDS spectra in any of the data from the TEM. If the W is incorporated with the KNN powder, as measured with DC plasma emission spectroscopy, then it is below the minimum detectability level. The other possibility is that the W is localized and was not found in the very small regions analyzed by the TEM.

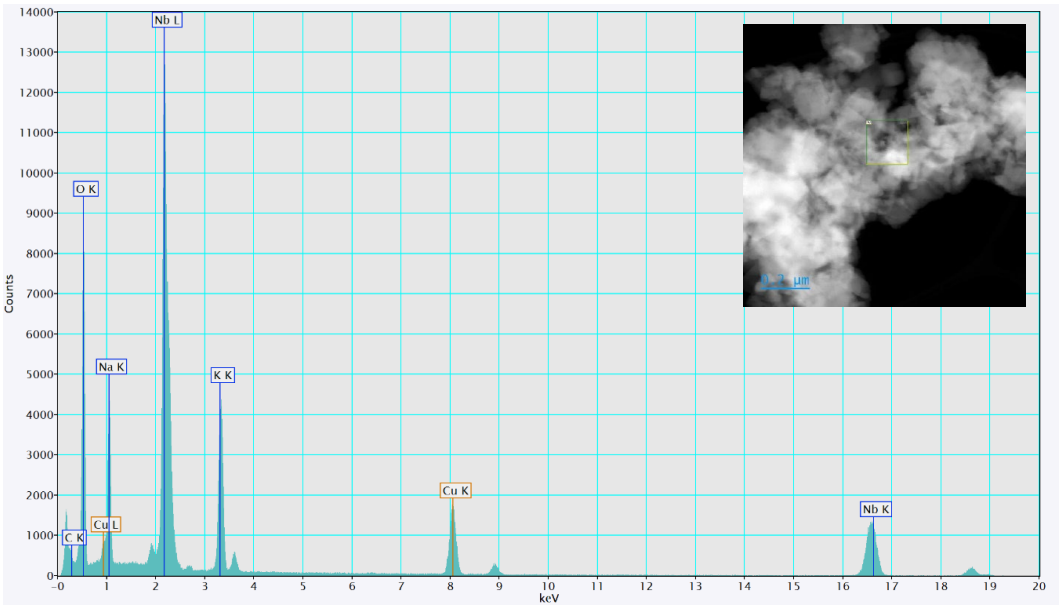

Fig. 7 XEDS spectrum from the indicated area (in red) showing the elements found in the synthesized KNN powder. The Cu-K peak is from the copper support grid and the C-K is mostly from the support film.

It is well-known that there is difficulty in determining the oxygen concentration with XEDS. However, the ratio of the higher atomic number elements determined from the composition using the Cliff–Lorimer method[46] should be very good. Therefore, the ratios of the cation elements were considered when comparing chemistries.

Table 4 shows the elemental ratio results for XEDS data. The shaded rows are noted because the data were collected with higher X-ray counts, which leads to a higher statistical confidence. Also, the Analytical 1 data were measured in TEM mode where a higher number of particles were included, while the other results were from smaller areas with fewer particles. It is interesting to compare not only the results within the XEDS, but also to the DC plasma results. All the XEDS results show similar deficiency of the Nb relative to K and Na that was seen in the DC plasma results. The larger area analysis in Analytical 1 shows good agreement with the ratio of K/N being close to 1. However, the smaller regional analyses of the powders differ significantly in all the elemental ratios. This strongly indicates that there are chemical inhomogeneities within the powder sample that vary locally and should be investigated further.

Table 4 Elemental ratio results for XEDS data of the synthesized KNN

Measurement	K/Na	K/Nb	Na/Nb
Anal. 1	0.96	1.03	1.08
Anal. 2	0.66	0.76	1.16
Anal. 3	0.62	0.79	1.28
Anal. 4	0.71	0.87	1.23
Anal. 5	0.75	0.99	1.33
Anal. 8	1.11	0.76	0.69
Anal. 9	0.92	0.83	0.90
SI Data(1)	0.74	0.59	0.80
SI Data(2)	0.79	0.87	1.09

Future studies investigate the influence of this simple incorporation of W into KNN through the simple ball-milling process on the piezoelectric and dielectric characteristics of the synthesized material. To better understand the implications of the incorporation of W into the synthesized KNN powder, one needs to get back to the basis of the functionality of KNN. As it is well known, KNN assumes an orthorhombic symmetry. The phase rich in K+ has the *Amm*2 polar group and the phase rich in Na^+ is assigned to monoclinic symmetry with the *Pm* polar group. It has been demonstrated that there is an internal dipole moment due to non-centrosymmetric space groups in niobate-based perovskites, resulting in separate centers of symmetry for the positive and negative charges.[47] The Nb displacement results in different bond lengths between the Nb and O atoms in the [NbO_6] octahedra.[48] It has been reported that the off-centered displacement of niobium atoms in the [NbO_6] octahedra leading to a boosted reactivity of the apical oxygen atoms result in the polarization and ferroelectricity in niobate-based perovskites.[49] There have been studies on incorporating anionic and cationic dopants into KNN to achieve improvements in electrical characteristics of the material[50–52] and that Sr_2C as a donor dopant in KNN improved its crystal structure, grain size, and phase composition.[53] With W being a donor dopant, and earlier reports outlining the benefits to the electrical properties by substituting other donor impurities such as strontium[53] and vanadium,[54] and the effects of W-doping on the piezoelectric performance of KNN is yet to be studied, the investigation of ferroelectric, dielectric, and piezoelectric characterization of the synthesized W-KNN would be highly interesting and beneficial.

As described in Section 2.2, the synthesized KNN powder was made into a compact using the hot-pressing technique. The resulting W-KNN disc was well sintered and robust as in Fig. 8c, with a diameter of 24.28 mm (Fig. 8a) and a thickness of 1.15 mm (Fig. 8b). The measured density using a gas pycnometer was 4.322 g/cm^3, which is a relative density of 95.8%. This number is consistent with additional measurements made using the Archimedes method. Notably, the color of the disc is dramatically different from the starting powder, having changed from a white

powder to a dark gray. This is likely due to a mixture of C diffusion into the sample, as well as O_2 vacancies created due to reactions between the powder and C, as well as the O_2-free atmosphere.[55] These defects may affect the piezoelectric performance of the hot-pressed samples, so further investigation is being performed to anneal the sintered parts in air to reintroduce O to the lattice.

Fig. 8 Well-sintered, dense compact made with synthesized W-KNN powder: (a) diameter, (b) thickness, and (c) relative size, related to a standard Sharpie

Ongoing are efforts to add contacts to these well-sintered dense compacts to pole and test for piezoelectric performance of the synthesized W-KNN and compare them to regular KNN to determine the effects of the incorporation of W cation dopant. Also ongoing are efforts to embed the W-KNN powder and regular KNN in a polymer to make flexible devices and characterize them for piezoelectric responses to vibrational and other forms of mechanical stimuli.

3. Conclusions

We report solvent-free mechanochemical synthesis of single-phase lead-free piezoelectric perovskite oxide (W-KNN) of KNN incorporated with W, using a simple high-energy ball-milling process with shorter processing times and lower calcination temperatures than those reported in literature and characterization of the derived powder using DC plasma emission spectroscopy, DSC, XRD, SEM, TEM, and XEDS. The results show the formation of crystalline KNN with traces of W. The presented method could also pave the way for a rapid, facile, and faster synthesis mechanisms at lower processing temperatures for other promising functional oxides.

The investigation of the impact of the incorporation of W in the KNN on piezoelectric, ferroelectric, and dielectric properties are ongoing efforts through the fabrication and testing of different types of devices with the synthesized W-KNN powder. W-KNN-based devices would enable lead-free, nontoxic, and environmentally friendly alternatives to current toxic lead-based piezoelectric devices for applications in actuation and sensing. Going forward, it would be interesting to investigate the nonlinear optoelectronic properties of the synthesized material to see how the Nb deficiency and the incorporation of W have affected the

bandgap and the resulting impact on sensing capabilities. In addition, the consequences of maturing biocompatible piezoelectrics such as KNN and improved application-specific fine-tuned variations of such materials could be transformational for applications such as biomedical prosthetics like bone implants.

4. References

1. Saito Y, Takao H, Tani T, Nonoyama T, Takatori K, Homma T, Nagaya T, Nakamura M. Nature. 2004;432:84.
2. Tkach A, Santos A, Zlotnik S, Serrazina R, Okhay O, Bdikin I, Costa ME, Vilarinho PM. Effect of solution conditions on the properties of Sol–Gel derived potassium sodium niobate thin films on platinized sapphire substrates. Nanomaterials. 2019;9:1600.
3. Abdullah AM, Sadaf MUlK, Tasnim F, Vasquez H, Lozano K, Uddin MJ. KNN based piezo-triboelectric lead-free hybrid energy films. Nano Energy. 2021;86:106133.
4. Bai Y, Kistanov AA, Wei C, Jari J. J Phys Chem C. 2021;125(16):8890–8898.
5. Jitena C, Rawatb M, Bhattacharyab A, Sing KC. (Na0.5K0.5)NbO3 nanocrystalline powders produced by high energy ball milling and corresponding ceramics. Mater Res Bull. 2017;90:162–169.
6. Jaffe B, Cook WR, Jaffe H. Piezoelectric ceramics. Academic Press; 1971.
7. Wolny WW. European approach to development of new environmentally sustainable electroceramics, Ceram Int. 2004;30:1079–1083.
8. Ringgaard E, Wurlitzer T. Lead-free piezoceramics based on alkali niobates. J Eur Ceram Soc. 2005;25:2701–2706.
9. Shrout T, Zhang S. Lead-free piezoelectricceramics: alternatives for PZT? J Electroceramics. 2007;19:111–124.
10. Sopicka-Lizer M. High-energy ball milling. Woodhead Publishing Limited; 2010.
11. Rödel J, Jo W, Seifert KTP, Anton E-M, Granzow T, Damjanovic D. Perspective on the development of lead-free piezoceramics. J Am Ceram Soc. 2009;92:1153–1177.
12. Baláž P, Achimovičová M, Baláž M, Billik P, Cherkezova-Zheleva Z, Criado JM, Delogu F, Dutková E, Gaffet E, Gotor FJ, et al. Hallmarks of mechanochemistry: from nanoparticles to technology. Chem Soc Rev. 2013;42:7571–7637.
13. Jeon JH. Mechanochemical synthesis and mechanochemical activation-assisted synthesis of alkaline niobate-based lead-free piezoceramic powders. Curr Opin Chem Eng. 2014;3:30–35.

14. Zhang Q, Saito F. A review on mechanochemical syntheses of functional materials. Adv Powder Technol. 2012;23:523–531.

15. Suryanarayana C. Mechanical alloying and milling. Prog Mater Sci. 2001;46:1–184.

16. Da Silva KL, Menzel D, Feldhoff A, Kübel C, Bruns M, Paesano A Jr, Düvel A, Wilkening M, Ghafari M, Hahn H, et al. Mechanosynthesized BiFeO3 nanoparticles with highly reactive surface and enhanced magnetization. J Phys Chem C. 2011;115:7209–7217.

17. Liu L, Wu M, Huang Y, Fang L, Fan H, Dammak H, Pham Thi M. Effect of mechanical activation on the structure and ferroelectric property of Na0.5K0.5NbO3. Mater Res Bull. 2011;46:1467–1472.

18. Rojac T, Kosec M, Malič B, Holc J. Mechanochemical synthesis of NaNbO3, KNbO3 and K0.5Na0.5NbO3. Sci Sinter. 2005;37:61–67.

19. Rojac T, Kosec M, Połomska M, Hilczer B, Šegedin P, Bencan A. Mechanochemical reaction in the K2CO3-Nb2O5 system. J Eur Ceram Soc. 2009;29:2999–3006.

20. Rojac T, Kosec M, Malič B, Holc J. The mechanochemical synthesis of NaNbO3 using different ball-impact energies. J Am Ceram Soc. 2008;91:1559–1565.

21. Ohara A, Kondo S, Shimoda H, Sato K, Abe H, Naito M. Rapid mechanochemical synthesis of fine barium titanate nanoparticles. Mater Lett. 2008;62:2957–2959.

22. Kong LB, Ma J, Huang H, Zhang RF, Que WX. Barium titanate derived from mechanochemically activated powders. J Alloys Compd. 2002;337:226–230.

23. Kuscer D, Holc J, Kosec M. Formation of 0.65Pb(Mg1/3Nb2/3)O3-0.35PbTiO3 using a high-energy milling process. J Am Ceram Soc. 2007;90:29–35.

24. Kong LB, Ma J, Zhu W, Tan OK. Preparation of PMN-PT ceramics via a high-energy ball milling process. J Alloys Compd. 2002;236:242–246.

25. Junmin X, Wang J, Weibeng N, Dongmei W. Activation-induced pyrochlore-to-perovskite conversion for lead magnesium niobate precursor. J Am Ceram Soc. 1999;82:2282–2284.

26. Kuscer D, Sturm ET, Kovac J, Kosec M. Characterization of the amorphous and the nanosized crystallites in high-energy milled lead-magnesium-niobate powder. J Am Ceram Soc. 2009;92:1224–1229.

27. Kuscer D, Holc J, Kosec M. Mechano-synthesis of lead-magnesium-niobate ceramics. J Am Ceram Soc. 2006;89:3081–3088.

28. Kong LB, Ma J, Zhu W, Tan OK. Preparation of PMN powders and ceramics via a high-energy ball milling process. J Mater Sci Lett. 2001;20:1241–1243.

29. Kong LB, Ma J, Huang H, Zhang RF. Effect of excess PbO on microstructure and electrical properties of PLZT7/60/40 ceramics derived from a high-energy ball milling process. J Alloys Compd. 2002;345:238–245.

30. Kong LB, Ma J, Zhu W, Tan OK. Preparation and characterization of PLZT ceramics using high-energy ball milling. J Alloys Compd. 2001;322:290–297.

31. Xue J, Wan D, Lee SE, Wang J. Mechanochemical synthesis of lead zirconate titanate from mixed oxides. J Am Ceram Soc. 1999;82:1687–1692.

32. Kong LB, Ma J, Zhang TS, Zhu W, Tan OK. Pb(ZrxTi1−x)O3 ceramics via reactive sintering of partially reacted mixture produced by a high-energy ball milling process. J Mater Res. 2001;16:1636–1643.

33. Kong LB, Zhu W, Tan OK. Preparation and characterization of Pb(Zr0.52Ti0.48)O3 ceramics from high-energy ball milling powders. Mater Lett. 2000;42:232–239.

34. Kong LB, Ma J, Zhu W, Tan OK. Preparation and characterization of lead zirconate ceramic from high-energy ball milled powder. Mater Lett. 2001;49:96–101.

35. Kong LB, Zhu W, Tan OK. PbTiO3 ceramics derived from high-energy ball milled nano-sized powders. J Mater Sci Lett. 2000;19:1963–1966.

36. Singh R, Patro PK, Kulkarni AR, Harendranath CS. Synthesis of nano-crystalline sodium niobate ceramic using mechanochemical activation. Ceram Int. 2014;40:10641–10647.

37. Rojac T, Benčan A, Kosec M. Mechanism and role of mechanochemical activation in the synthesis of (K, Na, Li)(Nb, Ta)O3 ceramics. J Am Ceram Soc. 2010;93:1619–1625.

38. Shrivastava A, Sakthivel S, Pitchumani B, Rathore AS. A statistical approach for estimation of significant variables in wet attrition milling. Powder Technol. 2011;211:46–53.

39. Lee G-J, Park E-K, Yang S-A, Park J-J, Bu S-D, Lee M-K. Rapid and direct synthesis of complex perovskite oxides through a highly energetic planetary milling. Sci Rep. 2017;7:46241. doi:10.1038/srep46241.

40. Shrout TR, Zhang SJ. Lead-free piezoelectric ceramics: alternatives for PZT? J Electroceram. 2007;19:111–124.

41. Quintero MC, Rincón M, Osorio-Guillén JM, López D, Londoño FA. Grinding methods effects on the synthesis of potassium sodium niobate powders by oxide mixing. TecnoLógicas, 2019;22(46):15–23.

42. Rutkowski P, Huebner J, Grabo´s A, Kata D, Sapiński B, Faryna M. Dense KNN polycrystals doped by Er_2O_3 obtained by hot pressing with hexagonal boron nitride protective layer. Materials. 2020;13(24):5741.

43. Bharathi P, Varma KBR. Effect of the addition of B_2O_3 on the density, microstructure, dielectric, piezoelectric and ferroelectric properties of K0.5Na0.5NbO3 ceramics. J Electron Mater. 2013;43:493–505.

44. ASTM E 1097-12. Standard guide for determination of various elements by direct current plasma atomic emission spectrometry. ASTM International; 2017 July 3.

45. Rojac T, Kosec M, Šegedin P, Malič B, Holc J. The formation of a carbonato complex during the mechanochemical treatment of a Na2CO3-Nb2O5 mixture. Solid State Ion. 2006;177:2987–2995.

46. Cliff G, Lorimer GW. The quantitative analysis of thin specimens. J of Microscopy. 1975;103(2):203–207.

47. Li L, Salvador PA, Rohrer GS. Photocatalysts with internal electric fields. Nanoscale. 2014;6:24–42.

48. Lanfredi S, Darie C, Bellucci FS, Colin CV, Nobre MAL. Phase transitions and interface phenomena in the cryogenic temperature domain of a niobate nanostructured ceramic. Dalton Trans. 2014;43:10983–10998.

49. Matos J, Lanfredi S, Montaña R, Nobre MAL, de Córdoba MCF, Ania CO. Photochemical reactivity of apical oxygen in KSr2Nb5O15 materials for environmental remediation under UV irradiation. J Colloid Interface Sci. 2017;496:211–221.

50. Lin D, Kwok KW, Chan HWL. Dielectric and piezoelectric properties of K0:50Na0:50NbO3–BaZr0:050Ti0:950O3) lead-free ceramics. Appl Phys Lett. 2007;91:143513.

51. Hussain F, Khesro A, Muhammad R, Wang D. Effect of Ta-doping on functional properties of K0.51Na0.49NbO3. Mater Res Expr. 2019;6:106309.

52. Hussain F, Khesro A, Lu Z, Alotaibi N, Mohamad AA, Wang G, Wang D, Zhou D. Acceptor and donor dopants in potassium sodium niobate based ceramics. Front Mater. 2020;7:160.

53. Hreščcak J, Dražić G, Deluca M, Arèon I, Kodre A, Dapiaggi M, Rojac T, Malič B, Bencan A. Donor doping of K 0.5 Na 0.5 NbO 3 ceramics with strontium and its implications to grain size, phase composition and crystal structure. J Eur Ceramic Soc. 2017;37:2073–2082.

54. Jiten C, Singh KC. Effect of vanadium substitution on electrical and piezoelectric properties of lead-free (K0.5Na0.5)NbO3 ceramics. J Mater Sci: Mater Electron. 2017;28:507–513.

55. Schlup AP, Costakis WJ, Rheinheimer W, Trice RW, Youngblood JP. Hot-pressing platelet alumina to transparency. J Am Ceram Soc. 2019;103(4):2587–2601. doi:10.1111/jace.16932.

List of Symbols, Abbreviations, and Acronyms

Al_2O_3	alumina
Ar	Argon
ARL	Army Research Laboratory
COD	Crystallography Open Database
DC	direct current
DSC	differential scanning calorimetry
h-BN	hexagonal boron nitride
JCPDS	Joint Committee on Powder Diffraction Standards
KNN	(K, Na) NbO_3, potassium sodium niobate
PZT	$PbZr_{(1-x)}Ti_xO_3$
SAED	selected area electron diffraction
SEM	scanning electron microscopy
STEM	scanning transmission electron microscopy
TEM	transmission electron microscope
TG	thermogravimetric
WC	tungsten carbide
W-KNN	lead-free piezoelectric perovskite oxide
XEDS	energy-dispersive X-ray spectroscopy
XRD	X-ray diffraction